

SCIENTIFIC REPORTS

OPEN

Reabsorption cross section of Nd³⁺-doped quasi-three-level lasers

Fei Chen¹, Junjie Sun¹, Renpeng Yan² & Xin Yu²

The ${}^4F_{3/2} \rightarrow {}^4I_{9/2}$ laser transition of Nd³⁺-doped crystals emitting at 900 nm is a standard quasi-three-level laser system. The reabsorption effect is one of the factors that restricts laser output power. Based on rate equations, a theoretical model considering the reabsorption effect for continuous-wave Nd³⁺-doped quasi-three-level lasers is established. The simulation results indicate that the reabsorption effect should be restrained to improve laser characteristics, which are mainly influenced by the Nd³⁺-doping concentration, laser medium length, pumping beam divergence angle and output mirror transmissivity. The optimal experimental results illustrate the availability of a theoretical model that considers the reabsorption effect. To quantitatively evaluate the reabsorption effect of a Nd³⁺-doped laser medium, a reabsorption cross section is proposed for the first time to the best of our knowledge. Comparing the experimental results and theoretical calculation results, the reabsorption cross section is estimated for a 912-nm Nd:GdVO₄ laser, 914-nm Nd:YVO₄ laser and 946-nm Nd:YAG laser.

High-power Nd³⁺-doped lasers operating at approximately 900 nm have been extensively studied because of their unique applications. First, 900-nm lasers with high power are efficient sources that can pump Yb-doped fibers and crystals to obtain a laser at approximately 980 nm¹. Second, these lasers are used for ozone measurements and remote sensing in water-vapor lidars and differential-absorption lidars. Moreover, these lasers are capable of generating blue lasers by frequency doubling^{2–5}. Many studies have been performed to achieve high-power Nd³⁺-doped lasers by employing various media and crystals, including Nd:YAG, Nd:YVO₄ and Nd:GdVO₄. In 1987, a 946-nm Nd:YAG laser was demonstrated for the first time⁶. Zhou *et al.* demonstrated a 8.3-W laser at 946 nm using a Nd:YAG rod in 2005⁷. In the same year, J. Gao realized a 25.4-W laser at 946 nm with a thin disk Nd:YAG crystal⁸. In 2017, Y. Sun reported a 946-nm Nd:YAG Q-switched laser with an achieved pulse energy of 2.63 mJ with a 10.8-ns pulse width and a peak power of approximately 244 kW⁹. A 914-nm laser in a Nd:YVO₄ crystal was reported by P. Zeller and P. Peuser in 2000 with a maximum output power of 3.0 W and a slope efficiency of 22.8%¹⁰. In 2009, W. Gong reported a V-shaped cavity that emitted a 7.3-W laser at 914 nm¹¹. In 2016, P. Jiang demonstrated an efficient 914-nm Nd:YVO₄ laser under double-end polarized pumping, and a 17.7-W continuous wave output was obtained with an efficiency of 33.4%¹². In a Nd:GdVO₄ crystal, a 912-nm laser with an output power of 8.0 W was achieved by X. Yu *et al.* in 2008¹³. In 2009, Y. F. Lv reported a Nd:GdVO₄ laser with an optical efficiency of 58.2% and a slope efficiency of 67.9%, corresponding to an output power of 8.1 W¹⁴. Afterwards, a novel indium-solder technology was demonstrated by R. P. Yan to improve the performance of a 912-nm Nd:GdVO₄ laser¹⁵.

The operation of 900-nm lasers in Nd³⁺-doped crystals is a standard quasi-three-level laser system because the lowest laser level is the uppermost component of the five crystal-field components of the ground-state ${}^4I_{9/2}$ level. A quasi-three-level laser system is different from the traditional four-level and three-level laser systems but has the characteristics of both. Achieving a high-power 900-nm laser in Nd³⁺-doped crystals is challenging. The main challenge can be ascribed to the nature of a quasi-three-level laser. On the one hand, the stimulated-emission cross section of the transition is small. On the other hand, the thermal population on the lowest laser level at room temperature will lead to a significant reabsorption effect¹⁶. The concept of the reabsorption effect in quasi-three-level lasers was proposed by T. Y. Fan and R. L. Byer in 1987⁶. W. P. Risk modeled longitudinally pumped solid-state lasers, including reabsorption loss, in 1988¹⁶, and this model could be employed to analyze laser characteristics, such as threshold and slope efficiency. Since 1988, the reabsorption effect has attracted more attention^{17,18}. A quasi-three-level laser output performance is seriously influenced by the reabsorption effect. Therefore, a method to quantitatively evaluate the reabsorption effect is indispensable for completing quasi-three-level laser theory.

¹State Key Laboratory of Laser Interaction with Matter, Innovation Laboratory of Electro-Optical Technology, Changchun Institute of Optics, Fine Mechanics and Physics, Chinese Academy of Sciences, Changchun, 130033, China. ²National Key Laboratory of Science and Technology on Tunable Laser, Harbin Institute of Technology, Harbin, 150080, China. Correspondence and requests for materials should be addressed to F.C. (email: feichenny@126.com)

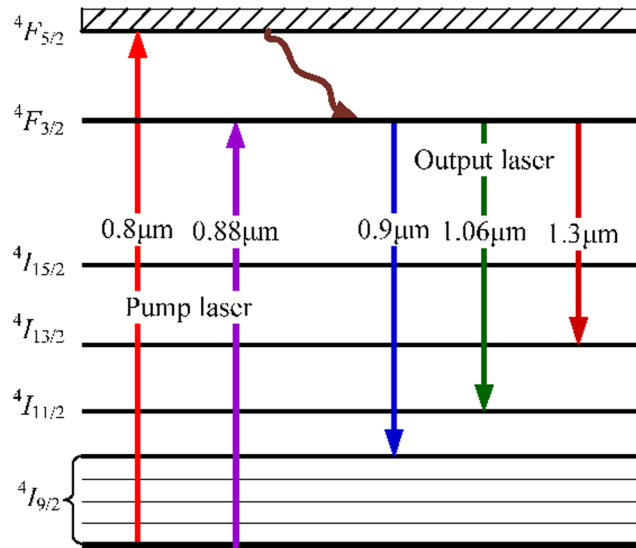


Figure 1. Energy-level diagram and laser emissions of Nd³⁺ crystals.

In this paper, a reabsorption cross section for evaluating the reabsorption effect of Nd³⁺-doped quasi-three-level lasers is proposed for the first time. Theoretical calculations considering the reabsorption effect suggest that the output performance is mainly influenced by the Nd³⁺-doping concentration, laser medium length, pumping beam divergence angle and output mirror transmissivity. In this experiment, Nd³⁺-doped quasi-three-level lasers using different Nd³⁺-doped laser media with high output power are realized. The experimental results correspond well to the simulation results considering the reabsorption effect. The numerical values of the reabsorption cross sections of a 912-nm Nd:GdVO₄ laser, 914-nm Nd:YVO₄ laser and 946-nm Nd:YAG laser were determined by comparing the theoretical and experimental results.

Results

Theoretical model. Figure 1 shows the energy levels and laser emissions of Nd³⁺ crystals. Nd³⁺ crystals with a large absorption cross section correspond to pump laser wavelengths of 800 nm and 880 nm. Laser output of approximately 1060 nm and 1300 nm operates between $4F_{3/2} \rightarrow 4I_{11/2}$ and $4F_{3/2} \rightarrow 4I_{13/2}$, respectively. The other transition $4F_{3/2} \rightarrow 4I_{9/2}$ is a quasi-three-level transition, and the lowest level is the uppermost level of the five branches of the ground state $4I_{9/2}$ energy level. For example, a laser operating at 912 nm is a quasi-three-level laser system, and the wave number of the lower level is 408 cm⁻¹. Assuming the number of thermal population particles of $4I_{9/2}$ level is N_L , and the ratio of the particles number of Z_5 branches to the total number in the ground state is f_1 . Therefore, the number of particles occupying the lower thermal level is $N_1 = f_1 N_L$. Similarly, the thermal population particles number of $4F_{3/2}$ is N_U , and the proportion of the particles number under the branch is f_2 , thus, the particles number in the upper thermal level is $N_2 = f_2 N_U$.

The relationship between f_1 and the operating temperature of the laser medium for Nd:GdVO₄, Nd:YVO₄ and Nd:YAG is shown in Fig. 2. At room temperature, the ratio of the number of thermal population particles on the Z_5 sublevel of the total number of ground states in Nd:GdVO₄, Nd:YVO₄ and Nd:YAG is 5.7%, 5% and 0.8%, respectively. The difference is caused by the different wave numbers of the lowest levels, i.e., 408 cm⁻¹, 433 cm⁻¹ and 857 cm⁻¹, respectively. Figure 2 shows that the number of particles, f_1 , in the quasi-three-level laser system linearly increases as the temperature increases. The laser reabsorption effect on the $4F_{3/2} \rightarrow 4I_{9/2}$ level transition will influence laser characteristics, such as the threshold power and output slope efficiency of a laser. Thus, lasers need to operate at temperatures as low as possible.

The analysis of the performance of a Nd³⁺-doped quasi-three-level laser considering the reabsorption effect begins with the rate equation. Pumping and oscillating lasers are assumed to be circularly symmetric TEM₀₀ Gaussian beams. Supposing that the density of inverse particles is $\Delta N(r, z) = N_2(r, z) - N_1(r, z)$, Equation (1) describes the density change of the upper and lower energy levels of Nd³⁺-doped lasers, where $\Delta N^0 = N_2^0 - N_1^0$ is the pump under the action of the inverse particle density number, τ stands for the laser-level life, c is the speed of light in a vacuum, σ is the laser-stimulated emission cross section, n is the laser refractive index of the medium, z is a coordinate in the direction of the laser axis, and r is a radial coordinate.

$$\frac{d\Delta N(r, z)}{dt} = (f_1 + f_2)R_p r_p(r, z) - \frac{\Delta N(r, z) - \Delta N^0}{\tau} - \frac{(f_1 + f_2)c\sigma \Delta N(r, z)}{n} \Phi \phi(r, z) = 0 \tag{1}$$

R_p represents the rate at which particles are emitted to the upper level in the pump and can be expressed as $R_p = P_{in}\eta/h\nu_p$, where P_{in} is the incident pump power, $\eta = 1 - \exp(-\alpha l)$ is the absorption rate of the laser medium with a length of l and absorption coefficient of α , h is the Planck constant and ν_p is the frequency of the pumping light. The number of photons in the laser cavity can be expressed as $\Phi = 2nlP_L/c\nu_L$, where P_L is the

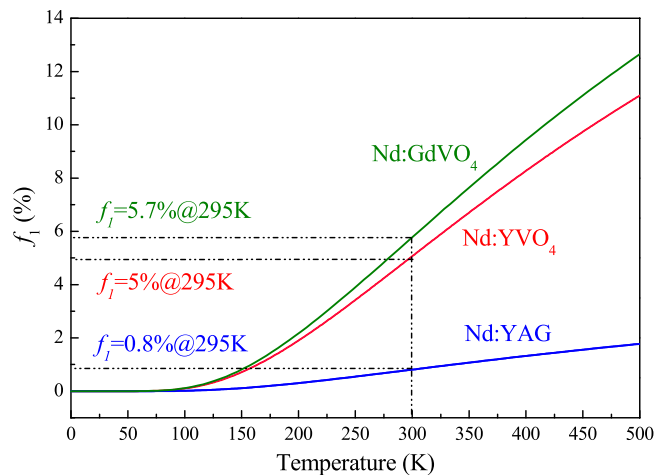


Figure 2. f_1 versus the working temperature of the laser medium.

dynamic laser power in one direction of the cavity and ν_L is the laser frequency. Equation (2) presents the number of reversed particles above the threshold, where $f^* = f_1 + f_2$.

$$\Delta N(r, z) = \frac{\tau f^* R_p r_p(r, z) - N_1^0}{1 + \frac{c\sigma_L}{n} f^* \Phi \phi(r, z)} \quad (2)$$

For the analysis of a Nd^{3+} -doped laser, the parameters were defined as follows. $a = \omega_p/\omega_L$ is the ratio of the waist radius of the pump beam to the waist radius of the oscillating beam, and $B = 2N_1^0\sigma l/(L + T)$ is the ratio of the reabsorption loss to the intrinsic loss of the laser cavity. $F = 4P_{in}\tau\sigma\eta/\pi h\nu_p\omega_L^2(L + T)$ is a parameter proportional to the incident pump power, and $S = 2c\sigma\tau\Phi/n\pi\omega_L^2 l$ is a parameter proportional to the power of the lasing laser. ω_p and ω_L are the waist radii of the pump beam and the laser beam, respectively. L is the loss of one round-trip of the cavity, and T is the transmissivity of the output mirror. Therefore, the slope efficiency, dP_{out}/dP_{in} , of the output laser light can be expressed as

$$\frac{dP_{out}}{dP_{in}} = \frac{T\nu_L\eta}{(L + T)\nu_p(f_1 + f_2)^2 F^2} \frac{1 + \frac{B}{(f_1 + f_2)S} \ln[1 + (f_1 + f_2)S]}{\int_0^\infty \frac{\left[\exp(-x) - \frac{Ba^2}{(f_1 + f_2)F} \exp(-2a^2x) \right]}{[1 + (f_1 + f_2)S \exp(-a^2x)]^2} dx} \quad (3)$$

where $x = 2r^2/\omega_p^2$. From Equation (3), we can obtain the numerical relationship between the output power of a Nd^{3+} -doped quasi-three-level laser and the pump power. The theoretical analysis shows that reabsorption has a remarkable influence on the output power and slope efficiency of Nd^{3+} -doped quasi-three-level lasers¹⁹.

Simulations and analysis. According to the theoretical model considering the reabsorption effect, calculated results for the Nd:GdVO_4 laser, Nd:YVO_4 laser and Nd:YAG laser were obtained employing the parameters in Table 1.

912-nm Nd:GdVO_4 laser calculation. The calculation results of the relationship between the output power of a 912-nm Nd:GdVO_4 laser with different parameters are depicted in Fig. 3. Figure 3(a) shows the output power as a function of the incident pump power considering different reabsorption effects, and the ratio of the waist radius of the pump beam to the laser beam is $a = 1.0$. The output power of the 912-nm laser is strongly influenced by the reabsorption effect. The output power decreases from 19.8 W to 5.08 W as B increases from 0 to 5.0 at a pump power of 70 W.

An optimum doping concentration and crystal length can improve laser characteristics. Additionally, the output power and slope efficiency of a laser are influenced by these parameters. Figure 3(b) shows the calculated results for the output power versus the doping concentration and crystal length. The Nd:GdVO_4 laser crystal with a doping concentration of 0.1 at.% and a length of 6–7 mm is optimal to obtain a 912 nm laser with power up to 14.7 W.

Using the above optimization parameters, the relationship between the output power and the transmissivity of the output mirror, T , is shown in Fig. 3(c). When $L = 0.01$, the optimum transmissivity of the output mirror is approximately 6%. When $L = 0.05$, the optimum transmissivity of the output mirror is approximately 10%. With an increase in L , the laser output power rapidly decreases because the laser emission cross section of a 912-nm quasi-three-level system decreases, leading to low laser gain. Additionally, the output power is greatly influenced by cavity loss. Therefore, to achieve high efficiency output from a 912-nm laser, the coating quality of the resonator mirror must be improved and the cavity loss must be reduced as much as possible. Figure 3(d) shows the

Parameter	Nd:GdVO ₄	Nd:YVO ₄	Nd:YAG
f_1 Fraction of the population density in the lowest laser level	0.5050	0.5055	0.51
f_2 Fraction of the population density in the upper laser level	0.0534	0.049	0.04
n Refractive index	1.973	1.973	1.816
τ Lifetime of the upper laser level	90	100	230
α Absorption coefficient	1.53	1.53	2.95
σ Stimulated-emission cross section	6.6×10^{-20}	4.8×10^{-20}	3.7×10^{-20}
ω_p Waist radius of the pump beam	200	200	200
ω_l Waist radius of the laser beam	200	200	200

Table 1. Main parameters of Nd³⁺-doped quasi-three-level lasers.

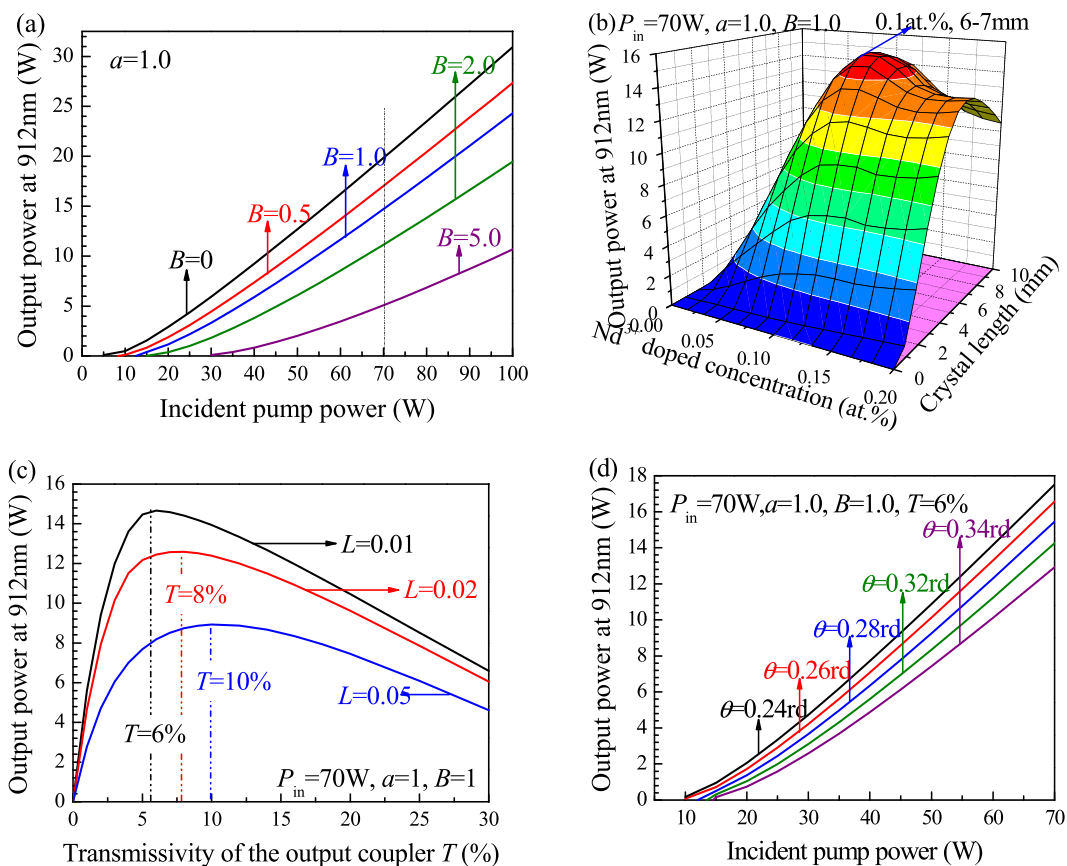


Figure 3. Output power of a 912-nm Nd:GdVO₄ laser versus (a) the pump power with different B . (b) Nd³⁺-doping concentration and length of the laser medium. (c) Transmissivity of the output coupler. (d) Incident pump power at different θ values.

output power versus the pump power at different divergence angles, θ . As the divergence angle, θ , decreases, the output power of the laser increases at the same injection pump power. Thus, the lens focal length used for the collimated focusing coupling system needs to be optimized to further increase the laser output power.

914-nm Nd:YVO₄ laser calculation. Similar to the 912-nm Nd:GdVO₄ laser system, the transition of the 914-nm Nd:YVO₄ laser belongs to a quasi-three-level laser system. The difference is that the wave number of the energy level in a 914-nm laser is 433 cm^{-1} . According to the theoretical model, the output power of a 914-nm Nd:YVO₄ laser versus different parameters was calculated. Figure 4(a) shows the 914-nm laser output performance considering different reabsorption effects at $\alpha=1.0$. When $P_{in}=70\text{ W}$, the maximum output power of the continuous laser decreases from 19.2 W to 9.05 W as B increases from 0 to 5.0. Figure 4(b) shows the relationship between the laser output power at 914 nm and the doping concentration and length of the laser medium at $P_{in}=70\text{ W}$. A Nd:YVO₄ laser with a doping concentration of 0.12 at.% and a length of 7–8 mm is optimal and can obtain a maximum output power of 17.2 W at 914 nm.

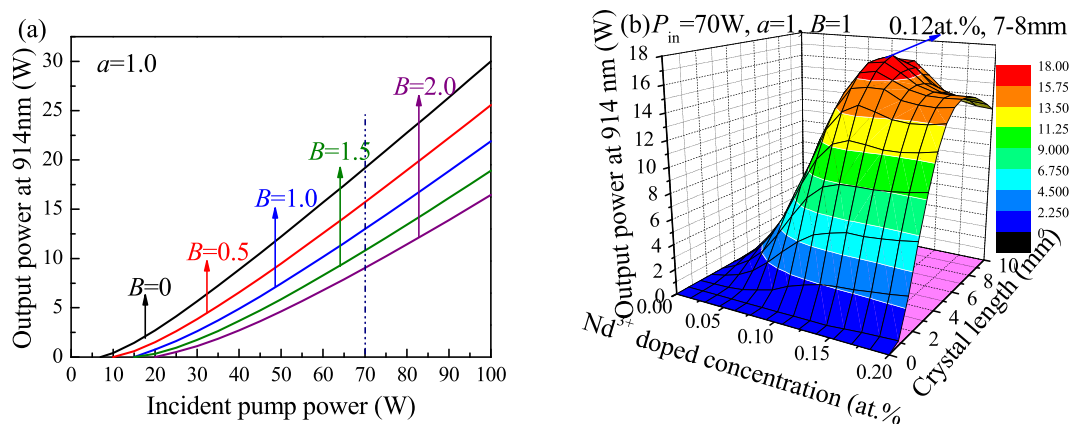


Figure 4. Output power of a 914-nm Nd:YVO₄ laser versus (a) the pump power with different B . (b) Nd³⁺-doping concentration and length of the laser medium.

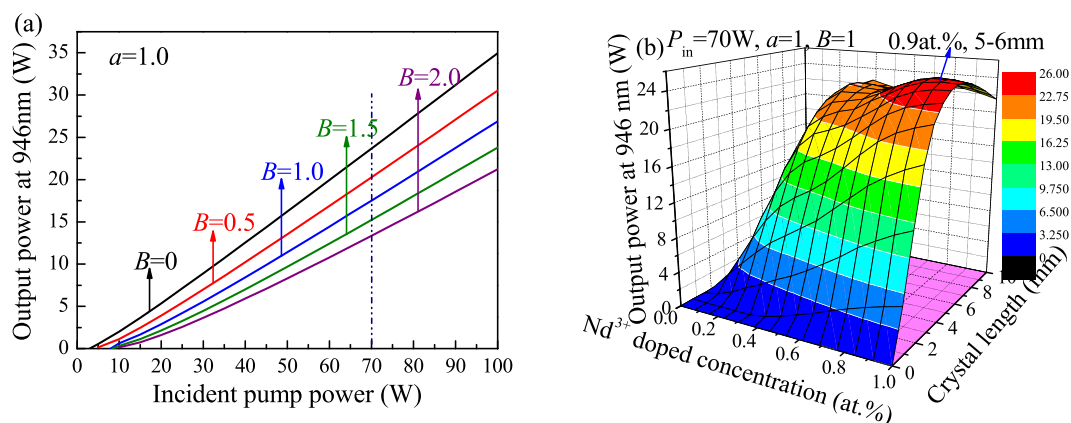


Figure 5. Output power of a 946-nm Nd:YAG laser versus (a) the pump power with different B . (b) Nd³⁺-doping concentration and length of the laser medium.

946-nm Nd:YAG laser calculation. The laser input-output curves of a 946-nm Nd:YAG laser considering different reabsorption effects are shown in Fig. 5(a). When $P_{in} = 70$ W, the maximum output power of the 946-nm continuous-wave laser decreases from 23.7 W to 13.3 W as B increases from 0 to 5.0. Figure 5(b) shows the relationship between the output power and the doping concentration and the length of the laser medium. The results suggest that a Nd:YAG laser crystal with a doping concentration of 0.9 at.% and a length of 5–6 mm can be used to realize a high-power-output 946-nm laser.

Experimental setup. To analyze the reabsorption effects of 912-nm Nd:GdVO₄ laser, 914-nm Nd:YVO₄ laser and 946-nm Nd:YAG laser, a diode-end-pumped quasi-three-level Nd³⁺-doped laser was employed, as shown in Fig. 6. The output light of the 808 nm LD (nLIGHT, Inc.) was coupled into the laser medium by a collimating focusing optical system, and the maximum output power of LD is 110 W. The laser media were provided by Castech Inc, and the surface of the crystal was coated with an antireflection film at 808–1340 nm. The crystals were mounted in a copper micro channel heat sink and maintained at 10 °C by water cooling. The reflecting mirror M1 was coated with a highly reflective film at approximately 900 nm ($HR > 99.9\%$) and a high-transmissivity film at 808 nm ($HT, T > 98\%$). The output mirror M2 partially transmitted at approximately 900 nm. To suppress the generation of four-level-laser parasitic oscillations, all mirrors were coated with a high-transmissivity film at 1063 nm and 1340 nm. The specifications of the filter are as follows: HT @ 900 nm ($T > 95\%$), HR @ 808 nm, 1063 nm ($T < 1\%$). The model of the power meter was PM30 (Coherent Inc., USA) with a response range of 0.19–11 μm and a maximum range and resolution of 50 W and 10 mW, respectively. For each crystal, the system was optimized with various parameters according to the theoretical calculations. Afterwards, the reabsorption cross section was determined by comparing the optimal results and the simulation results.

Evaluation of the reabsorption cross section. *912-nm Nd:GdVO₄ laser.* The high power output of the 912-nm Nd:GdVO₄ laser was obtained by optimizing parameters, which has been reported in Ref.¹⁹. The transmissivity of the output mirror was 6%; the doping concentration and length of the laser medium were 0.1 at.% and 6 mm, respectively. The output performance of 912-nm Nd:GdVO₄ laser was influenced by the spatial distribution of pump beam and laser beam in the crystal. The laser beam waist was fixed after optimizing the cavity structure.

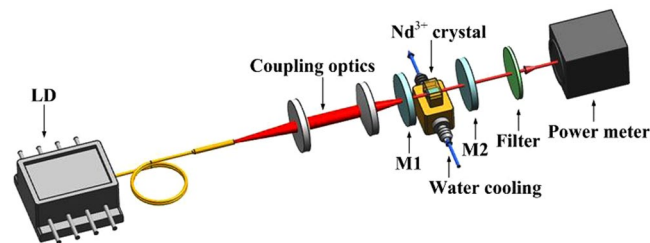


Figure 6. Diagram of the experimental setup for the quasi-three-level Nd³⁺-doped laser system.

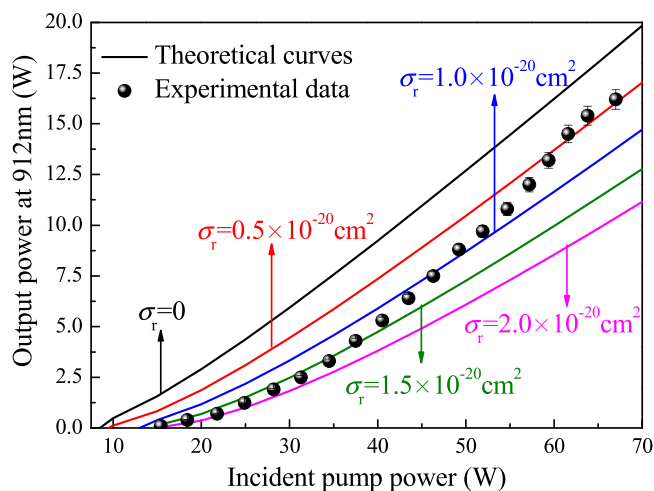


Figure 7. Comparison of the experimental results and the calculated curves of a 912-nm Nd:GdVO₄ laser.

Afterwards, the beam waist and the divergence angle of pump beam in the crystal were optimized by designing the coupling optics. The optimum parameters were as follows. The focal length of the collimation lens was 21.3 mm; and the ratio of the waist radius of the pump beam to the laser beam was $a = 1.0$. A maximum output power of 16.2 W was obtained with an optical conversion efficiency of 24.2% and an average slope efficiency of 41.7%. The experimental results are in good agreement with the theoretical calculation results, and the agreement verifies the validity of the theoretical simulation considering the reabsorption effect.

Therefore, to evaluate the reabsorption effect in Nd³⁺-doped laser media, the reabsorption cross section, σ_r , was defined and deduced from the excited emission cross section of the original rate equation. By comparing the theoretical calculation for the 912-nm laser output and the experimental results, the value of the reabsorption cross section, σ_r , of the 912-nm Nd:GdVO₄ laser was estimated.

As shown in Fig. 7, the input-output curves of the 912-nm Nd:GdVO₄ laser for different reabsorption cross sections were selected and compared with the experimentally measured values. It can be clearly seen that if the reabsorption effect is not taken into account, the output power curve greatly differs from the measured value. The laser threshold increases drastically due to the reabsorption effect. The reabsorption cross section of the 912-nm Nd:GdVO₄ laser was estimated to be $\sigma_r = (1.0 \pm 0.5) \times 10^{-20} \text{ cm}^2$.

The reabsorption effect is relevant to the number of particles on the lower energy level, and is dependent to the absorption of particles by pump laser. There are many particles being absorbed while the pump power is low, corresponding large reabsorption cross section, which leads high laser threshold. And the laser is unstable under low pump power, thus the rate of output power increasing is slow. While the pump power is high, the laser operation is stable. The rate of output power increasing gets fast. And there are less particles being absorbed by pump laser, corresponding to small reabsorption cross section.

914-nm Nd:YVO₄ laser. The optimization of the 914-nm Nd:YVO₄ laser system was similar to that of the 912-nm Nd:GdVO₄ laser system. Parameters, including the Nd³⁺-doping concentration, the length of the laser medium and the transmissivity of the output mirror, were optimized according to the theoretical calculation. As ref.²⁰ reported, the optimum length of the Nd:YVO₄ crystal is 6 mm with a Nd³⁺-doping concentration of 0.1 at.%, and the optimal transmissivity of the output mirror is $T = 6\%$. With an incident pump power of 67 W, an up to 15.5 W continuous wave 914-nm laser was obtained with an average slope efficiency of 37.6%. The calculated results were compared with the experimental results, as shown in Fig. 8. The reabsorption cross section of the 914-nm Nd:YVO₄ laser was estimated to be $\sigma_r = (0.5 \pm 0.5) \times 10^{-20} \text{ cm}^2$. This value is smaller than that of the Nd:GdVO₄ laser because the fraction of the population density in the lowest laser level of the Nd:GdVO₄ laser is greater, leading to a more serious reabsorption effect. The variation of reabsorption cross section with pump power is similar as 912-nm Nd:GdVO₄ laser.

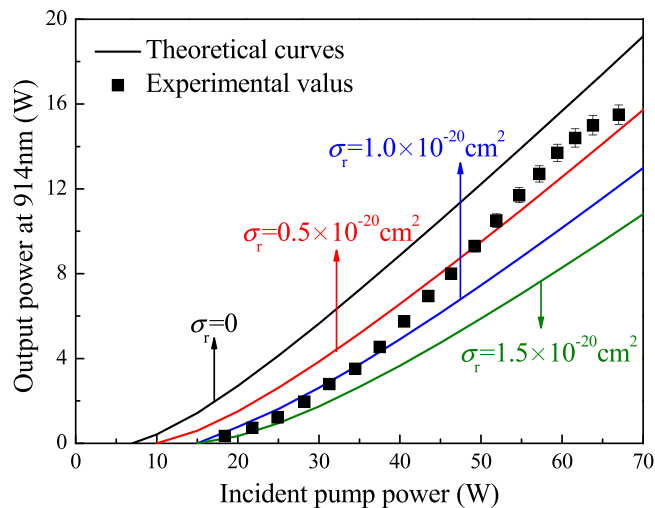


Figure 8. Comparison between the experimental results and the calculated curves for the 914-nm Nd:YVO₄ laser.

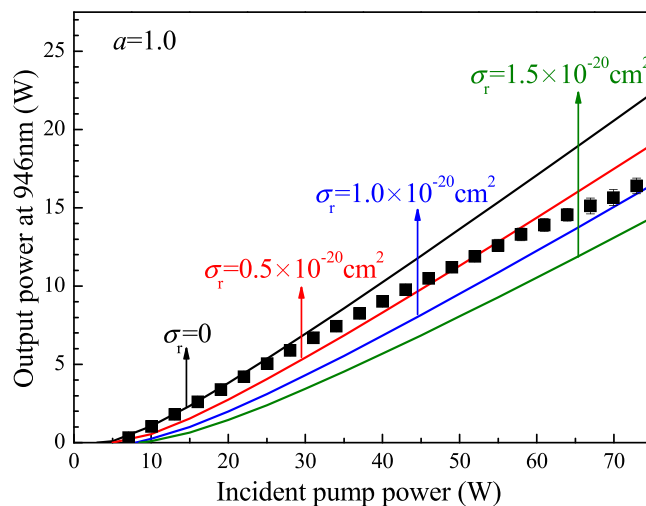


Figure 9. Comparison between the experimental results and the calculated curves for the 946-nm Nd:YAG laser.

946-nm Nd:YAG laser. Similarly, the 946-nm Nd:YAG laser was optimized as presented in ref.²¹. A 5-mm-length, 0.3-at.% Nd:YAG crystal was employed in the experiment, which deviated from the theoretical result. The reason for the deviation was the high absorption in the pump front end when a laser medium with a high doping concentration was used. When the 0.3-at.% 5-mm-length laser medium was employed, the output power and average slope efficiency were not the highest, but the laser output power grew linearly with the pump power. Furthermore, using the transmissivity, $T=9\%$, output coupler, a maximum output power of 17.2 W was obtained with a slope efficiency of 26.5%. The experimental results for the 946-nm Nd:YAG laser system were compared with the theoretical input-output curves, as shown in Fig. 9. In the experiment, the slope of the input-output curve decreased when the input power was greater than 50 W, which was inconsistent with the theoretical results. This inconsistency is ascribed to the use of a laser medium with a high doping concentration. The high absorption efficiency leads to the output laser tends to be saturated under high pump power. The reabsorption cross section of the 946-nm Nd:YAG laser is approximately $\sigma_r = (0.5 \pm 0.5) \times 10^{-20} \text{ cm}^2$.

Discussion

A reabsorption cross section was proposed to evaluate the reabsorption effect in a Nd³⁺-doped quasi-three-level system. Theoretical and experimental investigations of Nd³⁺-doped lasers were presented to determine the value of the reabsorption cross section. The effect of parameters, such as the transmissivity of the output mirror, doping concentration and length of laser medium, on a 912-nm Nd:GdVO₄ laser, 914-nm Nd:YVO₄ laser and 946-nm Nd:YAG laser was analyzed and theoretically calculated. In the experiments, the output power as a function of the input power was obtained using the optimal parameters, and the results were consistent with the theoretical

calculation results considering the reabsorption effect. The reabsorption cross section of the 912-nm Nd:GdVO₄ laser was estimated to be $(1.0 \pm 0.5) \times 10^{-20}$ cm² and was estimated to be $(0.5 \pm 0.5) \times 10^{-20}$ cm² for both the 914-nm Nd:YVO₄ laser and 946-nm Nd:YAG laser.

Methods

The analysis of the performance of Nd³⁺-doped quasi-three-level laser systems considering the reabsorption effect began with the rate equation. Parameters such as the doping concentration, length of the laser medium, transmissivity of the output mirror, cavity loss and divergence angle were considered to analyze how they influence the output power, threshold and slope efficiency of a laser. According to the theoretical analysis, simulations were performed to obtain the theoretical optimal parameters. Afterwards, the parameters were experimentally optimized, and the experimental results corresponded to the theoretical results. Finally, by comparing the theoretical results and optimal experimental results, the value of the reabsorption cross section was estimated.

References

1. Castaing, M. *et al.* Diode-pumped Nd:YVO₄/Yb:S-FAP laser emitting at 985 and 492.5 nm. *Opt. Lett.* **33**, 1234–1236 (2009).
2. Czeranowski, C., Heumann, E. & Huber, G. All-solid-state continuous-wave frequency-doubled Nd:YAG-BiBO laser with 2.8 W output power at 473 nm. *Opt. Lett.* **28**, 432–434 (2003).
3. Bjurshagen, S., Evekull, D. & Koch, R. Efficient generation of blue light by frequency doubling of a Nd:YAG laser operating on ⁴F_{3/2}-⁴I_{9/2} transitions. *Appl. Phys. B*, **76**, 135–141 (2003).
4. Gao, J. *et al.* Pulsed 456 nm deep-blue light generation by acousto optical Q-switching and intracavity frequency doubling of Nd:GdVO₄. *Laser Phys. Lett.* **5**, 577–581 (2010).
5. Zhou, R. *et al.* Q. Continuous-wave, 15.2 W diode-end-pumped Nd:YAG laser operating at 946 nm. *Opt. Lett.* **31**, 1869–71 (2006).
6. Fan, T. Y. & Byer, R. L. Modeling and CW operation of a quasi-three-level 946 nm Nd:YAG laser. *IEEE J. Quantum Electron.* **23**, 605–612 (1987).
7. Zhou, R. *et al.* 8.3 W diode-end-pumped continuous-wave Nd:YAG laser operating at 946 nm. *Opt. Express* **13**, 10115–10119 (2005).
8. Gao, J., Speiser, J. & Giesen, A. Diode-pumped continuous-wave quasi-three-level Nd:YAG thin disk laser. *Advanced Solid-State Photonics*, Tub **34** (2005).
9. Sun, Y. *et al.* 946 nm Nd:YAG double Q-switched laser based on monolayer WSe₂ saturable absorber. *Opt. Express* **25**, 21037–21048 (2017).
10. Zeller, P. & Peuser, P. Efficient, multiwatt, continuous-wave laser operation on the ⁴F_{3/2}-⁴I_{9/2} transitions of Nd:YVO₄ and Nd:YAG. *Opt. Lett.* **25**, 34 (2000).
11. Gong, W., Qi, Y. & Bi, Y. A comparative study of continuous laser operation on the ⁴F_{3/2}-⁴I_{9/2} transitions of Nd:GdVO₄ and Nd:YVO₄ crystals. *Opt. Commun.* **282**, 955–957 (2009).
12. Jiang, P. *et al.* Efficient 914 nm Nd:YVO₄ laser under double-end polarized pumping. *Appl. Opt.* **55**, 1072–1075 (2016).
13. Yu, X. *et al.* Diode-laser-pumped high efficiency continuous-wave operation at 912 nm laser in Nd:GdVO₄ crystal. *Laser Phys. Lett.* **6**, 34–37 (2009).
14. Lv, Y. F. *et al.* Highly efficient continuous-wave 912 nm Nd:GdVO₄ laser emission under direct 880 nm pumping. *Laser Phys. Lett.* **6**, 796–799 (2009).
15. Yan, R. P. *et al.* Improved performance of diode-end-pumped Nd:GdVO₄ 912 nm laser property with indium solder technology. *Laser Phys.* **21**, 462–467 (2011).
16. Risk, W. P. Modeling of longitudinally pumped solid-state lasers exhibiting reabsorption losses. *J. Opt. Soc. Am. B*, **5**, 1412–1423 (1988).
17. Zhang, C. *et al.* Modeling of actively Q-switched quasi-three-level lasers. *IEEE J. Quantum Electron.* **47**, 455–461 (2011).
18. Huang, J., Wan, Y. & Chen, W. Theoretical and experimental study on reabsorption effect and temperature characteristic of a quasi-three-level 946 nm Nd:YAG laser. *Proc. SPIE*, **9255** (2015).
19. Chen, F. *et al.* Theoretical and experimental investigations of a diode-pumped high-power continuous-wave 912 nm Nd:GdVO₄ laser operation at room temperature. *Opt. Commun.* **283**, 3755–3760 (2010).
20. Yu, X. *et al.* High power diode-pumped 914 nm Nd:YVO₄ laser. *Chin. Opt. Lett.* **8**, 000499–000501 (2010).
21. Chen, F. *et al.* Experimental investigation of a diode-pumped powerful continuous-wave dual-wavelength Nd:YAG laser at 946 and 938.6 nm. *Laser Phys.* **23**, 055002 (2013).

Acknowledgements

The authors acknowledge financial support from the National Defense Science and Technology Innovation Fund of the Chinese Academy of Sciences (Grant No. CXJJ-16M228), the Major Science and Technology Bidding Project No. 20160203016GX of Jilin Province, the Young and Middle-Aged Science and Technology Innovation Leader and Team Project No. 2017051901JH of Jilin Province, and the Youth Innovation Promotion Association of CAS.

Author Contributions

Fei Chen conducted the theoretical calculations and experiments. Junjie Sun, Renpeng Yan and Xin Yu analyzed the results. All authors reviewed the manuscript.

Additional Information

Competing Interests: The authors declare no competing interests.

Publisher's note: Springer Nature remains neutral with regard to jurisdictional claims in published maps and institutional affiliations.



Open Access This article is licensed under a Creative Commons Attribution 4.0 International License, which permits use, sharing, adaptation, distribution and reproduction in any medium or format, as long as you give appropriate credit to the original author(s) and the source, provide a link to the Creative Commons license, and indicate if changes were made. The images or other third party material in this article are included in the article's Creative Commons license, unless indicated otherwise in a credit line to the material. If material is not included in the article's Creative Commons license and your intended use is not permitted by statutory regulation or exceeds the permitted use, you will need to obtain permission directly from the copyright holder. To view a copy of this license, visit <http://creativecommons.org/licenses/by/4.0/>.

© The Author(s) 2019